# Effects of viscous dissipation and boundary conditions on forced convection in a channel occupied by a saturated porous medium

K. Hooman, H. Gurgenci

*School of Engineering, The University of Queensland, Brisbane, Australia*

**Abstract**. Forced convection with viscous dissipation in a parallel plate channel filled by a saturated porous medium is investigated numerically. Three different viscous dissipation models are examined. Two different sets of wall conditions are considered: isothermal and isoflux. Analytical expressions are also presented for the asymptotic temperature profile and the asymptotic Nusselt number. With isothermal walls, the Brinkman number significantly influences the developing Nusselt number but not the asymptotic one. At constant wall heat flux, both the developing and the asymptotic Nusselt numbers are affected by the value of the Brinkman number. The Nusselt number is sensitive to the porous medium shape factor under all conditions considered.

**Key words:** viscous dissipation, forced convection, channel, Brinkman-Brinkman problem

## Nomenclature

$a$ channel aspect ratio H/L

$Bn$ $\dfrac{\mu U^2}{k(T_m - T_w)}$

$Br$ Darcy-Brinkman number $\dfrac{\mu U^2 \varepsilon H^2}{k(T_i - T_w)K}$ for **T** and $\dfrac{\mu U^2 \varepsilon H}{q'' K}$ for **H**

$Br'$ clear fluid Brinkman number $\dfrac{Br}{S^2}$

$C_f$ boundary frictional drag coefficient

$c_P$ specific heat at constant pressure

$Da$ the Darcy number $Da = \dfrac{\mathrm{K}}{\varepsilon \mathrm{H}^2}$

$H$ half channel width

$k$ porous medium thermal conductivity

$K$ permeability

$L$ channel length

$Nu$ the Nusselt number

$p$ dimensionless pressure

$Pe$ the Péclet number $\dfrac{2\rho c_p UH}{k}$

$S$ $\left(\dfrac{\varepsilon \mathrm{H}^2}{\mathrm{K}}\right)^{\frac{1}{2}}$

$q''$ wall heat flux

$Re$ $\dfrac{2\rho UH}{\mu}$

$T$ temperature

$T_b$ bulk mean temperature

$T_{in}$ fluid inlet temperature

$T_w$ wall temperature

$u^*$ x-velocity

$u$ u*/U

$U$ inlet velocity

$v^*$ y-velocity

$v$ v*/U

$x^*$ longitudinal coordinate

$x$ x*/H

$y^*$ transverse coordinate

$y$ *y*/H*

**Greek symbols**

$\varepsilon$ porosity

$\theta$ dimensionless temperature $\frac{(T-T_W)}{(T_i-T_W)}$ *or* $k\frac{T-T_{in}}{q''H}$ for **T** or **H**

$\bar{\theta}$ modified asymptotic dimensionless temperature

$\theta_b$ dimensionless bulk temperature

$\mu$ fluid viscosity

$\rho$ fluid density

$\psi$ stream function

$\phi$ dimensionless viscous dissipation function

$\omega$ vorticity

## 1. Introduction

Flow through porous media is important in numerous engineering applications including geothermal energy, underground coal gasification and gas drainage, petroleum reservoirs, nuclear reactors, drying, environmental pollution, fuel cells, nano-manufacturing and nano-material processing. Nield and Bejan (2006) have presented a general review of the historical background of the developed models in porous media. It is known that the Brinkman flow model can predict

hydraulics through hyperporous media but the problem becomes mathematically complicated when the momentum transfer includes a viscous force term as first proposed by Brinkman (1947), and the thermal energy equation includes a viscous dissipation term involving a Brinkman number (Brinkman, (1951)). The term 'Brinkman-Brinkman' has been proposed for this problem by Nield (2006). Such Brinkman-Brinkman problems have been investigated by Ranjbar-Kani and Hooman (2004), and Hooman et al. (2006-b) where viscous dissipation was modeled by a velocity square term proposed by Bejan (1984). However, one knows that there are two other alternative viscous dissipation models (proposed by Al-Hadhrami et al. (2002,2003), and Nield (2002)) for a Brinkman-Brinkman problem. Haji-Sheikh et al. (2004) have reported a Green's function solution for the temperature distribution in a parallel plate channel applying the model proposed by Al-Hadhrami et al. (2003). Nield et al. (2003-a) and Kuznetsov et al. (2003) have considered each of the three models for the thermally developing region and solved the thermal energy equation applying a modified Graetz methodology. In a subsequent study, Nield et al. (2004) have revisited the problem by combining the three models into a single equation and solved the fully developed thermal energy equation for both isothermal and isoflux walls. These two wall conditions can also be referred to as **T** and **H** boundary conditions, respectively, in the terminology of Shah and London (1978).

However, in the light of Nield (2006), which was primarily a corrigendum to the paper by Nield et al. (2004), one thinks that a numerical solution can be a viable option to understand the physics of the problem where it can account for both the developing and the asymptotic case. Here, the development can be either thermally or hydrodynamically though the hydrodynamic development length is of order of magnitude $\left(\frac{\mathrm{K}}{\varepsilon}\right)^{\frac{1}{2}}$, where $K$ is the permeability and $\varepsilon$ is the porosity of the porous media. In most practical cases this is a small number and the problem is hydrodynamically fully developed through most of the flow region considered, for more details one can consult Nield and Kuznetsov (2005).

Another reason for seeking a numerical solution is that the thermally developing solutions presented for the Brinkman-Brinkman problems are of series type and one knows that such solutions should be checked for possible shortcoming of being of poor convergence behavior near the entrance (see for example Haji-Sheikh et al. (2006) where the authors paid special attention to the number of basis functions that they used in evaluating the solution in the near entry region at $x$/Pe=0.001).

Moreover, when it comes to apply the general model of Vafai and Tien (1981), to the authors' knowledge, there is no published work on comparing the models and our results might serve as a basis for an experimental test of the competing viscous dissipation models. Aiming at this goal and to make our results comparable to those of clear fluid case, we applied the general model of Vafai and Tien (1981) and neglected the Forchheimer term similar to Kaviany (1985). The conditions under which one can omit the so-called term are given in Vafai and Tien (1981). For more details one can consult Nield and Bejan (2006), Kaviany (1991), Hsu and Cheng (1990), and Whitaker (1999).

In addition to the traditional engineering applications such as simulation of highly viscous flows through porous journal bearings, the correct understanding of viscous dissipation in porous media transport is becoming more important with increased emphasis on analysis of micro- and nano-channel flow systems. As recently reviewed by Xu et al. (2002), with biomedical and lab-on-chip systems, better tools for modeling viscous dissipation are required due to the difficulty of ignoring viscous dissipation in such systems where high velocity gradients are present. Another interesting work was reported by Murakami and Mikic (2003) where the authors studied the effects of viscous dissipation on the optimum air-cooled micro-/narrow-channeled compact heat sink and concluded that the cooling capability under such conditions is largely limited by the salient manifestation of viscous dissipation, when compared with water-cooled systems. It was concluded that when a heat sink is to be designed with air, the effect of viscous dissipation should be taken into account in order to avoid falling on wrong optimum solutions. Another motivation

to present this work is the fact that some compact heat sinks can be modeled as a porous medium, as noted by Nield and Bejan (2006), and so the results could be applicable for such systems which are of current practical importance.

Previous work on the effects of viscous dissipation in ducts has been surveyed by Shah and London (1978) for the case of fluids clear of solid material and Magyari et al. (2005) for the case of a porous medium.

## 2. Analysis

### *2.1 Basic equations: primitive variables*

The fluid enters the channel at a uniform velocity/temperature being $U/T_{in}$. The channel is composed of two parallel plates 2H apart and each of them being held at either uniform temperature, $T_w$, or at uniform heat flux, $q''$, where the channel aspect ratio (defined as a=L/H) is fixed at a=8. Figure 1 shows the schematic view of the problem under consideration. It is assumed that the magnitude of the thermophysical properties are constant and that there is local thermal equilibrium. A criterion (that is met in most circumstances) for the validity of this assumption for steady forced convection was given by Nield (1998). Under these assumptions and by treating the solid matrix and the fluid as a continuum, the dimensionless governing equations for uniform porosity distribution are

$$\frac{\partial u}{\partial x}+\frac{\partial v}{\partial y}=0, \tag{1}$$

$$u\frac{\partial u}{\partial x}+v\frac{\partial u}{\partial y}=-\frac{\partial P}{\partial x}+\frac{2}{\mathrm{Re}}\left(\left(\frac{\partial^2 u}{\partial x^2}+\frac{\partial^2 u}{\partial y^2}\right)-S^2 u\right), \tag{2}$$

$$u\frac{\partial v}{\partial x}+v\frac{\partial v}{\partial y}=-\frac{\partial P}{\partial y}+\frac{2}{\mathrm{Re}}\left(\left(\frac{\partial^2 v}{\partial x^2}+\frac{\partial^2 v}{\partial y^2}\right)-S^2 v\right), \tag{3}$$

$$u\frac{\partial\theta}{\partial x}+v\frac{\partial\theta}{\partial y}=\frac{2}{Pe}\left(\left(\frac{\partial^2\theta}{\partial x^2}+\frac{\partial^2\theta}{\partial y^2}\right)+Br\phi\right), \quad (4)$$

where length, velocity, and pressure scales are H, U, and $\rho U^2$, respectively. There are two length scales for this problem being the pore-particle dimension $\left(\frac{\mathrm{K}}{\varepsilon}\right)^{\frac{1}{2}}$ and H. We applied the latter and introduced the porous media shape factor as $S=\left(\frac{\varepsilon\mathrm{H}^2}{\mathrm{K}}\right)^{\frac{1}{2}}$. Defining the Darcy number as $Da=\frac{\mathrm{K}}{\varepsilon\mathrm{H}^2}$, one verifies that $S=Da^{-1/2}$. The dimensionless temperature profile for **T** and **H** boundary conditions are defined as $\theta=\frac{T-T_w}{T_{in}-T_w}$ and $\theta=k\frac{T-T_{in}}{q''H}$, respectively. Other dimensionless parameters are defined in the nomenclature.

Following Nield et al. (2004), we combine the three alternative models into a single equation to find the dimensionless form of the viscous dissipation function as

$$\phi=u^2+v^2-\frac{c_1}{S^2}\left[u\left(\frac{\partial^2u}{\partial x^2}+\frac{\partial^2u}{\partial y^2}\right)+v\left(\frac{\partial^2v}{\partial x^2}+\frac{\partial^2v}{\partial y^2}\right)\right]+\frac{c_2}{S^2}\left[2\left(\left(\frac{\partial u}{\partial x}\right)^2+\left(\frac{\partial v}{\partial y}\right)^2\right)+\left(\frac{\partial v}{\partial x}+\frac{\partial u}{\partial y}\right)^2\right]. \quad (5)$$

where

(Model 1) for the Darcy model $c_1 = 0$ and $c_2 = 0$,

(Model 2, Nield) for the "power of drag force" model $c_1 = 1$ and $c_2 = 0$,

(Model 3, Al-Hadhrami et al. (2003)) for the "clear fluid compatible" model $c_1=0$ and $c_2=1$.

In each case the added Brinkman term is $O(S^{-2})$ compared to the Darcy term so that for large values of S the three models are effectively equivalent to each other.

Other models have been used in the past but the present selection of three is based on a critical review by Nield et al. (2004). One may consult Magyari et al. (2005), Hooman and Ejlali (2005), Hooman et al. (2006-a), and Nield and Hooman (2006) for more details.

*2.2 Vorticity-stream function formulation*

The vorticity-stream function method is applied to solve the set of equations (1-5). Taking the curl of the momentum equations 2-3, one finds that

$$\frac{\partial(u\omega)}{\partial x}+\frac{\partial(v\omega)}{\partial y}=\frac{2}{\mathrm{Re}}\left(\frac{\partial^2\omega}{\partial x^2}+\frac{\partial^2\omega}{\partial y^2}-S^2\omega\right) \quad , \tag{6}$$

where

$$\omega=-\left(\frac{\partial^2\psi}{\partial x^2}+\frac{\partial^2\psi}{\partial y^2}\right), \tag{7}$$

is the vorticity directed in z direction and the stream function, $\psi$, is defined as

$$u=\frac{\partial\psi}{\partial y}, \qquad v=-\frac{\partial\psi}{\partial x}. \tag{8-a,b}$$

One knows that in this way the continuity equation, equation 1, is satisfied identically.

The thermal energy equation now takes the following form

$$\frac{\partial(u\theta)}{\partial x}+\frac{\partial(v\theta)}{\partial y}=\frac{2}{Pe}\left(\frac{\partial^2\theta}{\partial x^2}+\frac{\partial^2\theta}{\partial y^2}+Br\phi\right). \tag{9}$$

The appropriate boundary conditions are shown in figure 1. More details of the vorticity-stream function method may be found in Tannehill et al. (1997).

Similar to Kaviany (1985) the boundary frictional drag coefficient, $C_f$, is defined as

$$C_f = \frac{4\mu \left.\frac{\partial u}{\partial y}\right|_{y=0}}{\rho U H}, \tag{10-a}$$

or in dimensionless form

$$C_f \,\mathrm{Re} = 4 \left.\frac{\partial u}{\partial y}\right|_{y=0}. \tag{10-b}$$

that may be referred to as the friction factor for short.

Following Nield and Bejan (2006), we define the Nusselt number, Nu, in terms of the channel width rather than the hydraulic diameter for **T** and **H** cases as

$$Nu_T = -2\frac{\left.\frac{\partial \theta}{\partial y}\right|_{y=0}}{\theta_b}, \qquad Nu_H = \frac{2}{\theta_w - \theta_b}, \tag{11-a,b}$$

where the dimensionless bulk mean temperature, independent of the thermal boundary condition, is defined as

$$\theta_b = \int_0^1 u\theta dy. \tag{12}$$

To compare this Nu with those based on the hydraulic diameter one should compare our Nu with Nu/2 of them as we will do hereafter.

## 3. Asymptotic temperature profile

Before presenting the developing solutions, an asymptotic solution is to be reported for the **T** boundary condition. Our aim is to apply this exact solution to verify our numerical results for very large values of x, i.e. when $x \to \infty$.

For the hydrodynamically fully developed problem there exists a unidirectional flow in the streamwise direction and the velocity distribution may be found as

$$u = \sigma\left(1 - \frac{\cosh S(y-1)}{\cosh S}\right), \tag{13-a}$$

where

$$\sigma = \left(1 - \frac{\tanh S}{S}\right)^{-1}. \tag{13-b}$$

For the asymptotic region, i.e. when $x \to \infty$, the thermal energy equation reduces to

$$\frac{d^2\theta}{dy^2} + Br\phi = 0, \tag{14-a}$$

with

$$\phi = u^2 + S^{-2}\left(c_2\left(\frac{du}{dy}\right)^2 - c_1 u\frac{d^2u}{dy^2}\right). \tag{14-b}$$

We define a new dimensionless temperature profile as

$$\bar{\theta} = \frac{\theta}{Br\sigma^2}. \tag{15}$$

Now the thermal energy equation reads

$$\frac{d^2\bar{\theta}}{dy^2} + 1 + \frac{1-c_1-c_2}{2\cosh^2 S} + (c_1-2)\frac{\cosh S(y-1)}{\cosh S} + \frac{1-c_1+c_2}{2\cosh^2 S}\cosh 2S(y-1) = 0, \tag{16}$$

where the appropriate boundary conditions are

$$\bar{\theta}(0) = 0, \qquad \frac{d\bar{\theta}}{dy}(1) = 0. \tag{17-a,b}$$

Finally one finds, by twice direct integration, that

$$\bar{\theta} = \left(1 + \frac{1-c_1-c_2}{2\cosh^2 S}\right)\frac{2y-y^2}{2} + (c_1-2)\frac{\cosh S - \cosh S(y-1)}{S^2\cosh S} + \left(1-c_1+c_2\right)\frac{\cosh 2S - \cosh 2S(y-1)}{8S^2\cosh^2 S} \tag{18}$$

Applying equation 12, one finds the bulk mean temperature as

$$\bar{\theta}_b = \left(1+\frac{1-c_1-c_2}{2\cosh^2 S}\right)\left(\frac{\sigma}{3}-\frac{1}{S^2}\right)+(2-c_1)\frac{\left(-3+\sigma\tanh^2 S\right)}{2S^2}+(1-c_1+c_2)\frac{\left((4-\sigma)\tanh^2 S+3\right)}{24S^2} \quad (19)$$

Equation 11-b is applied to find the asymptotic Nusselt number as

$$Nu = \frac{S^2\left(\frac{(3-c_1-c_2)}{\sigma}+(c_1+c_2-1)\tanh^2 S\right)}{\left(1+\frac{1-c_1-c_2}{2\cosh^2 S}\right)\left(\frac{\sigma S^2}{3}-1\right)+(2-c_1)\frac{\left(-3+\sigma\tanh^2 S\right)}{2}+(1-c_1+c_2)\frac{\left((4-\sigma)\tanh^2 S+3\right)}{24}} \quad (20)$$

Figure 2 presents the Nusselt number versus S for each of the three models. A quick check of this figure shows that as S approaches zero the three models converge towards different Nu values. Applying model 1, one finds Nu=3.862 at S=1 which is near to Nu=3.860 reported by Nield et al. (2003-a). For S=0, model 3, the clear fluid compatible model, leads to the same value reported by Ou and Cheng (1973-a), i.e. Nu=8.75. The differences between the models become smaller as S increases with all models converging towards a common plateau. For models 1 and 2, the Nusselt number increases as S increased and this is similar to the results of model 1 for flow through a circular tube (see for example figure 8 of Ranjbar-Kani and Hooman (2004)). For model 3, Nu initially decreases as S increases, passes through a minimum, and then increases. The minimum point for the clear fluid compatible model, model 3, is very close to the inflection points for the other models and occurs at $S \cong 2$ or $\sqrt{\frac{K}{\varepsilon}} \cong \frac{H}{2}$. The three models rapidly converge towards the same solution after this point where the macro scale (H/2) exceeds the micro one ($\sqrt{\frac{K}{\varepsilon}}$). A large value of S corresponds to the Darcy flow limit for which the three models are effectively the same. At S=10, for example, the Nusselt number is found to be 4.936, 5.123, and 5.193 for respective models. For very large values of S ($S \to \infty$) Nu tends to 6 which is in agreement with Hooman and Gorji-Bandpy (2005) and confirms Nu =5.953 reported by Nield et al. (2003-a).

**4. Numerical details**

In this study the computational domain is chosen to be larger than the physical one to eliminate the entrance and exit effects. The computational domain is symmetric above the horizontal mid-plane and therefore we consider the lower half of the flow region, shown in figure 1-b to reduce the computational time. Numerical solution for the governing equations for vorticity, stream function, and dimensionless temperature are obtained by finite difference methods, using the Gauss-Seidel technique with SOR. The governing equations are discretized by applying the second-order accurate central difference schemes. For the numerical integration, algorithms based on the trapezoidal rule are employed.

All runs were performed with a 30 x 200 grid. Grid independence was verified by running different combinations of S, Re, Br, and Pe on a 60 x 400 grid for both boundary conditions to observe that the result will not change to four significant figures. The convergence criterion (maximum relative error in the values of the dependent variables between two successive iterations) in all test runs was set at $10^{-6}$. Accuracy of the numerical procedure was verified by comparison of the results given in the literature, as shown in figure (3-4) and table 1.

Table 1 verifies our numerical results in three ways; versus the exact solution presented for **T** boundary condition by Nield et al. (2003-a), Haji-Sheikh et al. (2004), and also versus the asymptotic Nu obtained in the previous section (we fixed the Pe and Re value at Pe=5 and Re=2 in this work). Figures (3-a,b) are presented to compare the fully developed friction factor, and velocity profile of present study with those of Kaviany (1985) and Hooman and Merrikh (2006) (in fact with $0.5C_fRe$ of their results since they defined their Re in terms of the hydraulic diameter that is 2H when their aspect ratio tends to be very large). Figure (4) compares our results with those of Nield et al. (2004). To achieve this goal we relate their clear fluid Brinkman number, Bn, defined as

$$\mathrm{Bn} = \frac{\mu U^2}{k(T_m - T_w)}, \tag{21-a}$$

to our clear fluid Brinkman number, $Br'$, as follows

$$\mathrm{Bn} = -\frac{NuBr'}{2}. \tag{21-b}$$

Recasting the results of Nield et al. (2004), one finds that

$$\mathrm{Nu} = \frac{70}{17 + 27Br'}. \tag{22}$$

In the above equation $Br'$ is a clear fluid Brinkman number related to our Darcy-Brinkman number as $Br' = BrS^{-2}$. This form of Nu-Br correlation is similar to that reported for the clear fluid case. For example, Kakaç et al. (1987) reported the following Nu-Br correlation for fully developed flow through a pipe with **H** boundary condition

$$\mathrm{Nu} = \frac{48}{11 + 48Br}. \tag{23}$$

The above equation, similar to our equation 22, shows that Nu decreases with Br for positive values of Br. The reader should note that in both Nu and Br in the above equation the pipe diameter is selected as the length scale. A similar correlation is reported by Ou and Cheng (1973-b).

## 4. Results and discussion

### *4.1 Hydrodynamic aspects*

Figure 5 is presented to observe the hydrodynamic development by showing the streamwise velocity distribution versus x. Figures 5-a and 5-b correspond to S=1 and S=10, respectively. Based on these two figures one understands that for smaller values of S the hydrodynamic development length is larger, as expected. Not only the hydrodynamic development length but

also the fully developed velocity profile is affected by S in such a way that increasing S decreases the centerline velocity magnitude. A large value of S means that the pore scale is much smaller than the plate separation and the flow resembles the Darcy flow, with the velocity more or less uniform through the section with most of the variation occurring in a thin layer near the wall.

Figure 6 shows the friction factor versus x for S=1, and S=10. Increasing S increases the friction factor similar to what reported by Kaviany (1985). One also observes that the friction factor decreases with *x* and reaches a constant value in the fully developed region similar to the clear fluid case (see for example figure (3-2) of Bejan (1984)).

*4.2 Heat transfer aspects*

*4.2.1* ***T*** *boundary condition*

The Nusselt number is plotted against x for three viscous dissipation models and two shape factor values (S=1 and 10) in Figure 7 for a Darcy-Brinkman number of Br=1. At S=10, all three models behave similarly with the models 2 and 3 almost indistinguishable and model 1 slightly lower. This is similar to the trend observed for the asymptotic Nu values displayed for S>10 in Figure 3. On the contrary, for S=1, plot of model 3 stands above the other two with model 1 predicting the smallest Nu value. It is worth noting that only model 3 leads to the clear fluid Nu at very small S (8.75 as $S \to 0, x \to \infty$). Another feature of considerable interest is that for the smallest S value the Nusselt number predicted by model 3 is higher than those by other models even with higher S values.

Figures 8-a,b display equivalent results at a Darcy-Brinkman number of 10. For clarity, the results pertaining to small and large S are plotted separately. Figure 8-a displays the Nu-x variation for three models at S=1 and Figure 8b does the same for S=10. To complete the picture, the Nu-x plot for the case of no dissipation (Br=0) is also presented in figure 8-a. As seen, for large values of S, plots of both the developing and the asymptotic Nu for models 2 and 3 are

almost indistinguishable for any non-zero Br, however, for model 1 the developing Nu shows a decrease with a decrease in Br (though the asymptotic Nu is again independent of Br). It is observed that moving from Br=1 to Br=10 slightly affects Nu. However, it is known that moving from a problem without dissipation to another one with even an small Br changes the nature of the fully developed problem, as mentioned in previous reports (see Nield and Hooman (2006) for a list of the articles). Though for all of the three models the asymptotic Nu is independent of Br, for the developing region a decrease in Nu is observed when Br is increased for small S values.

*4.2.2 **H** boundary condition*

Figure 9 shows the developing Nusselt number in the absence of viscous dissipation, i.e. when Br=0. The trend shown here is similar to that reported by Nield et al. (2003-b). Figure 10 illustrates the developing Nusselt number for S=10 where the three models show similar trends. One observes that the results of the entrance region are qualitatively similar to those of **T** boundary condition.

Figure 11 presents the Nusselt number versus x for S=1 with Br=0.1. Considering the fully developed region, models 1 and 2 lead to nearly an equal Nu value while model 3 predicts a 3.649 value for Nu. This value is close to the clear fluid result based on equation 22 which is Nu=3.553. Though the fully developed Nu values of models 1 and 2 are very close, in the developing region plot of model 2 stands near that of model 3 at the channel entry. Moving downstream the channel, plots of models 1 and 2 merge to each other in such a way that in the fully developed region the Nusselt numbers become very close with that of model 1 standing over the other counterpart.

## 5. Conclusion

The effect of viscous dissipation on both developing and asymptotic heat transfer in a parallel plate channel filled with a porous medium, has been studied, both for uniform-temperature and uniform-flux boundary conditions. The effect of various viscous dissipation models on the thermal aspects of the problem has been investigated. It is observed that, regardless of the boundary condition, the three models lead to similar Nu values when S is large, however, when it comes to small S values only model 3 claims to be valid. This can also be expressed in terms of the physical dimensions in such a way that when the micro scale becomes large enough to be comparable to the macro dimensions, the differences between the three models become negligible.

**Acknowledgments**

The first author, the scholarship holder, acknowledges the support provided by The University of Queensland in terms of UQILAS, Endeavor IPRS, and School Scholarship.

**References**

Al-Hadhrami, A.K., Elliott, L., Ingham, D.B.: 2002, Combined free and forced convection in vertical channels of porous media, *Transport Porous Media*, **49**, 265-289.

Al-Hadhrami, A.K., Elliott, L., Ingham, D.B.: 2003, A new model for viscous dissipation in porous media across a range of permeability values, *Transport Porous Media*, **53**, 117-122.

Bejan, A.: 1984, *Convection Heat Transfer*, Wiley, New York.

Brinkman, H.C.: 1947, On the permeability of media consisting of closely packed porous particles. *Appl. Sci.Res. A* **1**, 81-86.

Brinkman, H.C.: 1951, Heat effects in capillary flow. *Appl. Sci.Res. A* **2**, 120-124.

Haji-Sheikh, A., Minkowycz, W.J., Sparrow, E.M.: 2004, Green's function solution of temperature field for flow in porous passages, *Int. J. Heat Mass Transfer*, **47**, 4685-4695.

Haji-Sheikh, A., Nield, D.A., Hooman, K.: 2006, Heat transfer in the thermal entrance region for flow through rectangular porous passages, *Int. J. Heat Mass Transfer*, **49**, 3004–3015.

Hooman, K., Ejlali A.: 2005, Second law analysis of laminar flow in a channel filled with saturated porous media: a numerical solution, *Entropy*, **7**, 300-307.

Hooman, K., Gorji-Bandpy, M.: 2005, Laminar dissipative flow in a porous channel bounded by isothermal parallel plates, *Appl. Math. Mech.-Engl. Ed.*, **26**, 578-593.

Hooman, K., Merrikh, A.A.: 2006, Analytical solution of forced convection in a duct of rectangular cross-section saturated by a porous medium, *ASME J. Heat Transfer*, **128**, 596-600

Hooman, K., Merrikh, A.A., Ejlali, A.: 2006a, Comments on "Flow, thermal, and entropy generation characteristics inside a porous channel with viscous dissipation" by S. Mahmud and R.A. Fraser, *Int. J. Thermal Sciences*, in press.

Hooman, K., Pourshaghaghy, A., Ejlali, A.: 2006b, Viscous dissipation effects on thermally developing forced convection in a porous saturated circular tube, *Appl. Math. Mech.-Engl. Ed*, **27**, 617-626.

Hsu, C.T., Cheng, P.: 1990, Thermal dispersion in porous medium, *Int. J. Heat Mass Transfer*, **33**, 1587-1597.

Kakaç, S., Shah, R.K., Aung, W.: 1987, *Handbook of Single-Phase Convective Heat Transfer*, Chapter 3, Wiley, New York

Kaviany, M.: 1985, Laminar flow through a porous channel bounded by isothermal parallel plates, *Int. J. Heat Mass Transfer*, **28**, 851-858.

Kaviany, M.: 1991, *Principles of Heat Transfer in Porous Media*, Springer-Verlag, New York.

Kuznetsov, A.V., Nield, D.A., Xiong, M.: 2003, Thermally developing forced convection in a porous medium: circular ducts with walls at constant temperature, with longitudinal conduction and viscous dissipation effects, *Transport Porous Media*, **53**, 331-345.

Magyari, E., Rees, D.A.S., Keller, B.: 2005, *Effect of viscous dissipation on the flow in fluid saturated porous media*, in Handbook of Porous Media (K. Vafai, ed.), 2nd ed., Taylor and Francis, New York, 373-407.

Murakami, Y., Mikic, B.B.: 2003, Parametric investigation of viscous dissipation effects on optimized air cooling microchanneled heat sinks, *Heat Transfer Engng*., **24,** 53-62.

Nield, D.A.: 1998, Effects of local thermal non-equilibrium in steady convective processes in a saturated porous medium: forced convection in a channel. *J. Porous Media* **1**, 181-186.

Nield, D.A.: 2000, Resolution of a paradox involving viscous dissipation and nonlinear drag in a porous medium, *Transport Porous Media* **41**, 349-357.

Nield, D.A.: 2002, Modelling fluid flow in saturated porous media and at interfaces, in *Transport Phenomena in Porous Media II* (D. B. Ingham and I . Pop, eds.), Elsevier Science, Oxford.

Nield, D.A.: 2004, Comments on 'A new model for viscous dissipation in porous media across a range of permeability values' by A. K. Al-Hadhrami, L. Elliot and D. B. Ingham, *Transport Porous Media*, **55**, 253-254.

Nield, D.A.: 2006, A note on a Brinkman-Brinkman forced convection problem, *Transport Porous Media*, **64**, 185-188

Nield, D.A., Bejan, A.: 2006, *Convection in Porous Media*, 3rd ed., Springer-Verlag, New York.

Nield, D.A., Hooman, K.: 2006, Comments on "Effects of viscous dissipation on the heat transfer in forced pipe flow. Part 1: both hydrodynamically and thermally fully developed flow, and Part 2: thermally developing flow" by O. Aydin, *Energy Conv. Manag.*, **47**, 3501-3503.

Nield, D.A., Kuznetsov, A.V.: 2005, *Forced convection in porous media: transverse heterogeneity effects and thermal development*, in Handbook of Porous Media (K. Vafai, ed.), 2nd ed., Taylor and Francis, New York, 143-193.

Nield, D.A., Kuznetsov, A.V., Xiong, M.: 2003a, Thermally developing forced convection in a porous medium: parallel plate channel with walls at constant temperature, with longitudinal conduction and viscous dissipation effects, *Int. J. Heat Mass Transfer*, **46**, 643-651.

Nield, D.A., Kuznetsov, A.V., Xiong, M.: 2003b, Thermally developing forced convection in a porous medium: parallel plate channel or circular tube with walls at constant heat flux, *J. Porous Media*, **6**, 203-212.

Nield, D.A., Kuznetsov, A.V., Xiong, M.: 2004, Effects of viscous dissipation and flow work on forced convection in a channel filled by a saturated porous medium, *Transport Porous Media*, **56**, 351-367.

Ou, J.W., Cheng, K. C.: 1973a, Effects of pressure work and viscous dissipation on Graetz problem for gas flows in parallel-plate channels, *Wärme- und Stoffübertragung*, **6**, 191-198.

Ou, J.W., Cheng, K. C.: 1973b, Viscous Dissipation effects on thermal entrance region heat transfer in pipes with uniform wall heat flux, *Appl. Sci. Res.*, **28**, 289-301.

Ranjbar-Kani, A.A., Hooman, K.: 2004, Viscous dissipation effects on thermally developing forced convection in a porous medium: circular duct with isothermal wall, *Int. Comm. Heat Mass Transfer*, **31**, 897-907.

Shah, R. K., London, A. L.: 1978, *Laminar Flow Forced Convection in Ducts* (*Advances in Heat Transfer, Supplement 1*), Academic Press, New York.

Tannehill, J.C., Anderson, D.A., Pletcher, R. H.: 1997, *Computational Fluid Mechanics and Heat Transfer*, 2nd ed., Taylor & Francis.

Vafai, K., Tien, C.L.: 1981, Boundary and inertia effects on flow and heat transfer in porous media, *Int. J. Heat Mass Transfer*, **24**, 195-203.

Whitaker, S.: 1999, *The Method of Volume Averaging*, Dordrecht ; Boston, Kluwer Academic.

Xu, B., Ooi, K.T., Mavriplis, C., Zaghloul, M.E.: 2002 Viscous dissipation effects for liquid flow in Microchannels, in *Technical Proceedings of the International Conference on Modeling and Simulation of Microsystems*, Nanotech 2002, **1**, Chapter 2: Micro and Nano Fluidic Systems, 100-103.

**Tables 1:** The summary of the present and benchmark results for Nu (S=1).

**Figure captions:**

Figure 1-a,b Definition sketch

Figure 2 The asymptotic Nusselt number versus S.

Figure 3-a Comparison of fully developed velocity profile with that of Kaviany (1985)

Figure 3-b Comparison of fully developed friction factor ($C_f$Re) with that of Hooman and Merrikh (2006)

Figure 4 Code validation for the **H** boundary condition. (S=1)

Figure 5-a/b Streamwise velocity at some longitudinal locations (S=1)/(S=10).

Figure 6 The friction factor versus x for S=1 and S=10.

Figure 7 The Nusselt number versus x for S=1 and S=10 (Br=1).

Figure 8-a/b The Nusselt number versus x for S=10 (Br=0 and Br=10)/S=1 (Br=10).

Figure 9 The Nusselt number versus x for some values of S with Br=0.

Figure 10 The Nusselt number versus x for S=10 (Br=1).

Figure 11 The Nusselt number versus x for S=1 (Br=0.1).

Table 1 The summary of the present and benchmark results for Nu (S=1).

| Models | Present work Numerical/Exact | | Nield et al. (2003) | | Haji-Sheikh et al. (2004) | |
|---|---|---|---|---|---|---|
| | Br=0 | $Br \neq 0$ | Br=0 | $Br \neq 0$ | Br=0 | $Br \neq 0$ |
| 1 | 3.803 | 3.863/3.863 | 3.802 | 3.86 | 3.801 | - |
| 2 | | 4.162/4.162 | | 4.16 | | - |
| 3 | | 6.647/6.647 | | 6.641 | | 6.649 |

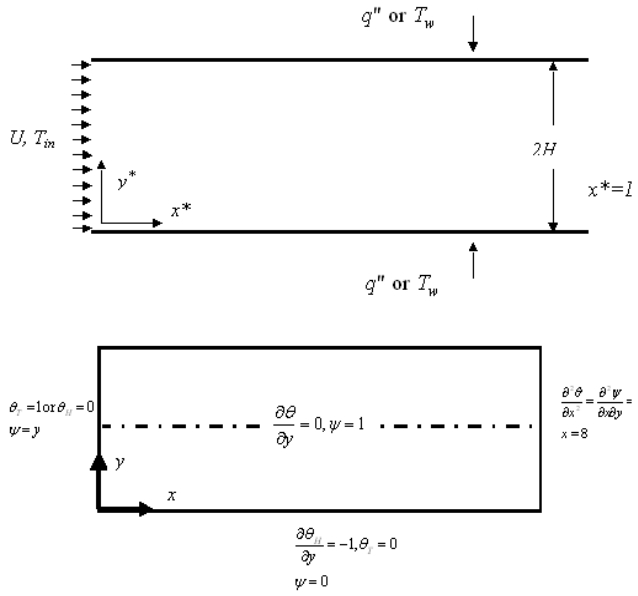


Figure 1-a,b Definition sketch

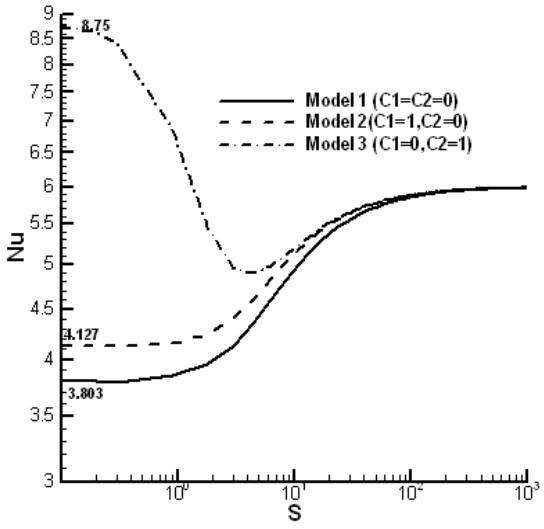


Figure 2 The asymptotic Nusselt number versus S.

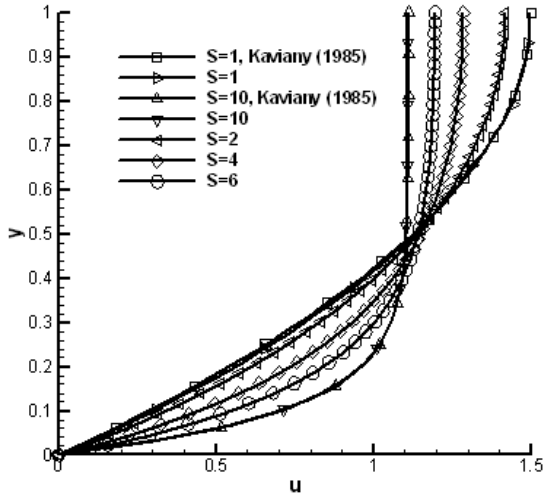


Figure 3-a Comparison of fully developed velocity profile with that of Kaviany (1985)

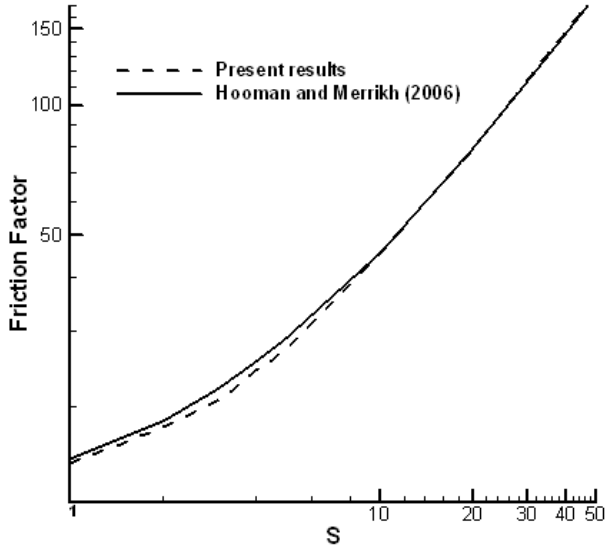


Figure 3-b Comparison of fully developed friction factor ($C_f$Re) with that of Hooman and Merrikh (2006)

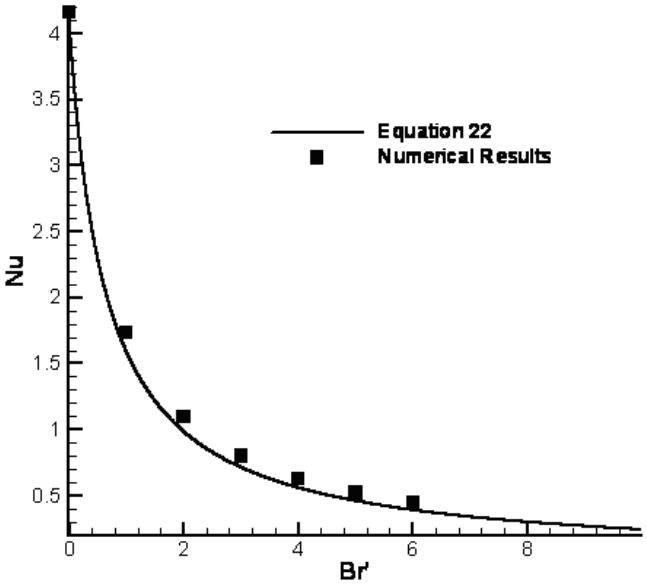


Figure 4 Code validation for the H boundary condition. (S=1)

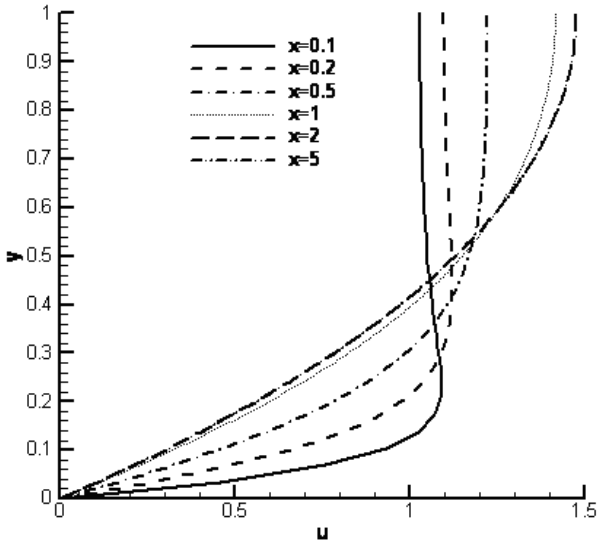


Figure 5-a Streamwise velocity at some longitudinal locations (S=1).

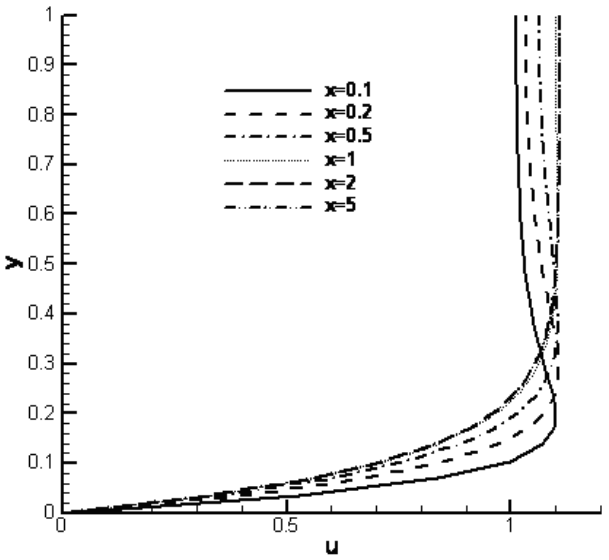


Figure 5-b Streamwise velocity at some longitudinal locations S=10.

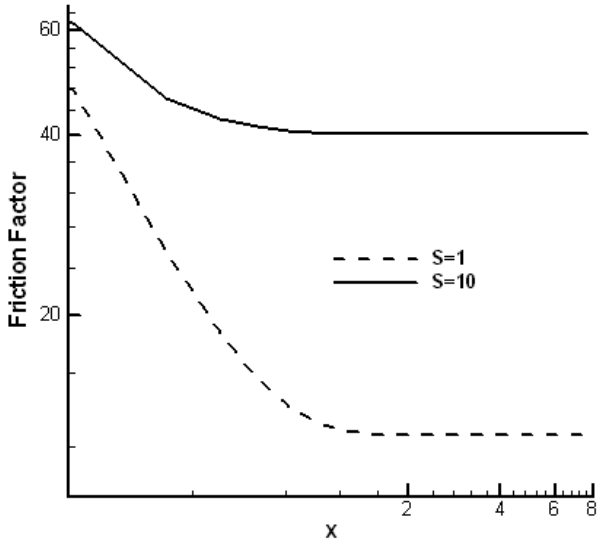


Figure 6 The friction factor versus x for S=1 and S=10.

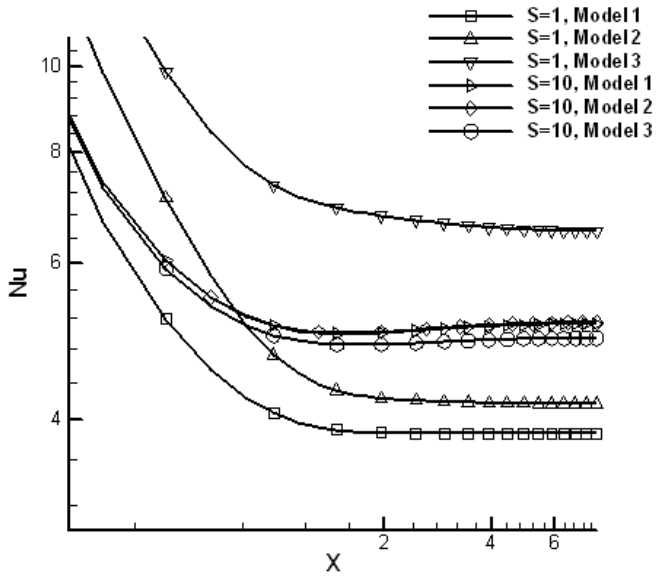


Figure 7 The Nusselt number versus x for S=1 and S=10 (Br=1).

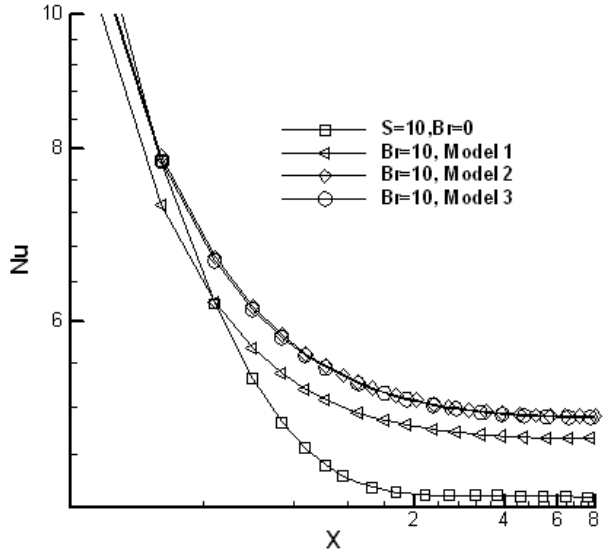


Figure 8-a The Nusselt number versus x for S=10 (Br=0 and Br=10).

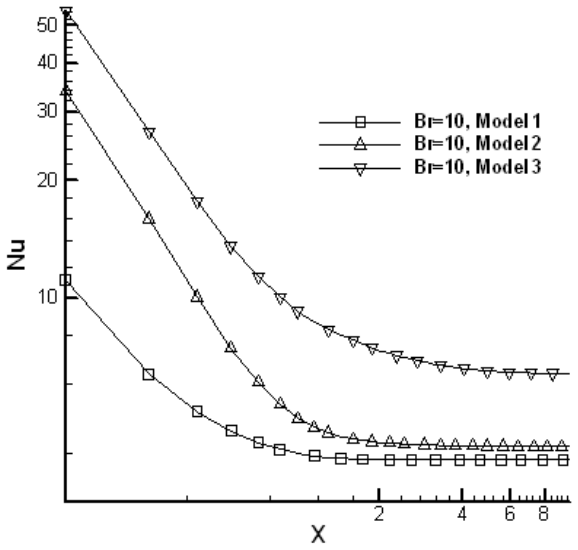


Figure 8-b The Nusselt number versus x for S=1 (Br=10).

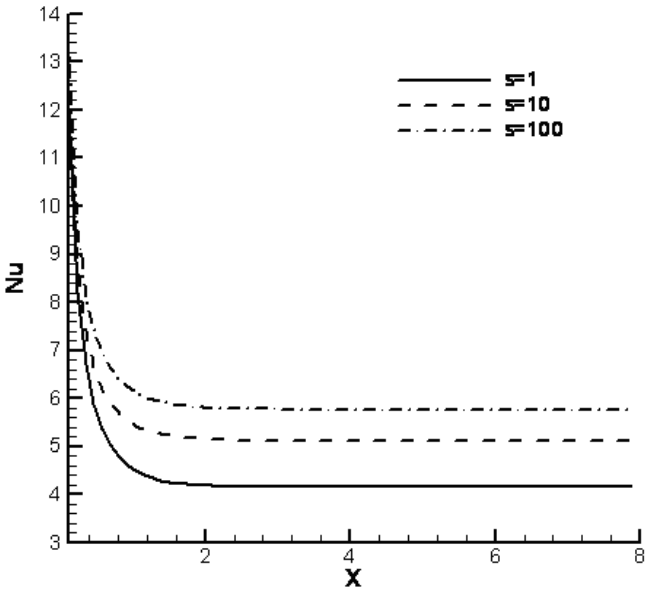


Fig. 9

Figure 9 The Nusselt number versus x for some values of S with Br=0.

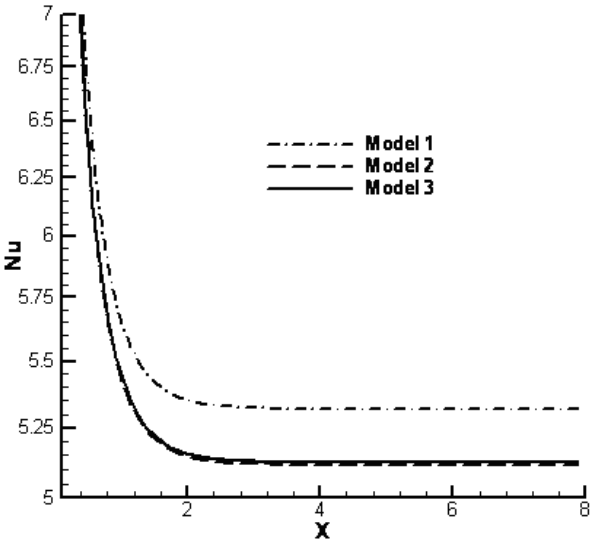


Fig. 10

Figure 10 The Nusselt number versus x for S=10 (Br=1).

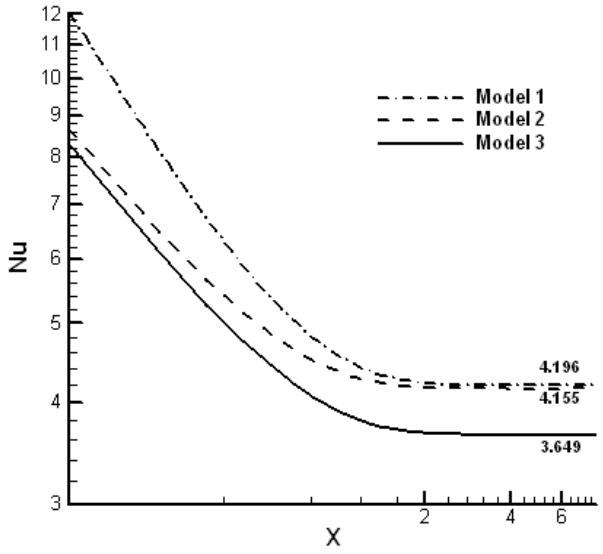


Figure 11 The Nusselt number versus x for S=1 (Br=0.1).